J Nanostruct 16(4): 5639-5651, Autumn 2026

RESEARCH PAPER

Preparation and In-vitro Evaluation of Spironolactone Loaded Transethosome Gel for Topical Application

Mustafa J. Muhana *, Abeer H. Khasraghi

Department of Pharmaceutics, College of pharmacy, University of Baghdad, Iraq

ARTICLE INFO

Article History:
Received 17 May 2026
Accepted 25 September 2026
Published 01 October 2026

Keywords:
Cold method
Ethanol injection
Lecithin
Spironolactone
Transethosomes

ABSTRACT

Spironolactone (SPL) is an aldosterone blocker with antiandrogen effects. It works by inhibiting 5α-reductase activity. The main objective of this research is to assess the safety and effectiveness of 0.25% topical spironolactone gel for managing acne vulgaris. SPL transethosomes(TEs) were prepared by the ethanol injection method and the cold method using lecithin and Phospholipon 90G as phospholipids, Tween 80, sodium deoxycholate and Span 80 as edge activators and cholesterol at different weights; TEs were further characterized by PS, PDI, zeta potential, encapsulation efficacy and dissolution study. The optimized formula was characterized by PXRD, DSC, FESEM, and FTIR. The optimized formula was formulated as a topical gel and further characterized by visual appearance, drug content, pH measurement, and rheology. The eighteen formulas were formulated with PS range (52.54nm to 5000nm; EE ranged from 29% to 99%; solid-state characterization of the SPL13 optimum formula showed amorphous formation; FTIR showed a broad peak due to the formation of a new hydrogen bond. In addition, all other peaks of SPL were retained, indicating no chemical interaction. The gel was successfully formulated and characterized; it was one-phase opaque, and the study of rheology showed a shear-thinning system. These results suggest that SPL-TEs can effectively enhance SPL dermal penetration in gel formulations.

How to cite this article
Muhana M., Khasraghi A. Preparation and In-vitro Evaluation of Spironolactone Loaded Transethosome Gel for Topical Application. J Nanostruct, 2026; 16(4):5639-5651. DOI: 10.22052/JNS.2026.04.094

INTRODUCTION

Over the past two decades, the field of drug delivery has advanced significantly as researchers develop new strategies to enhance therapeutic efficacy and minimize side effects. Lipid-based vesicular carriers are particularly prominent because of their biocompatibility, biodegradability, and ability to transport both hydrophilic and lipophilic drugs [1-3]. Among these, transethosomes (TEs), an innovative addition to vesicular drug delivery, hold great potential and overcome many limitations of conventional methods. These highly deformable lipid vesicles combine ethosomes' structural features with TEs flexibility. Since Song et al. introduced them in 2012, TEs have shown superior skin penetration and more efficient drug delivery than traditional carriers. Their composition, which includes phospholipids, ethanol, and edge activators, enables them to traverse biological barriers more effectively than liposomes or ethosomes.TEs are an advanced vesicle delivery system incorporating both an edge activator and

* *Corresponding Author Email: mostafa.jaber2400m@copharm.uobaghdad.edu.iq*

This work is licensed under the Creative Commons Attribution 4.0 International License.
To view a copy of this license, visit http://creativecommons.org/licenses/by/4.0/.

ethanol. They combine the benefits of ethosomes and deformable liposomes, providing enhanced penetration and deposition capabilities [4].The interaction between phospholipids and ethanol enhances drug permeation. Ethanol reduces the organization of the subcutaneous lipid layer, increasing its fluidity by lowering the melting temperature of this layer and disrupting the skin's lipid bilayer [5].

Lecithin was used as the main component of TEs because of its inherent characteristics, such as solubilizing substances with different physicochemical properties, biocompatibility, thermodynamic stability, thermoreversible nature, and resistance to microbial contamination [4].

The edge activator weakens the vesicle's double lipid layer, enhancing its flexibility and deformability. This allows the vesicles to pass through the pores of the stratum corneum. It increases bilayer deformability by affecting the interface voltage of the vesicles. Span 80, Tween 80, and sodium deoxycholate: These surfactants increase vesicle flexibility and deformability of the vesicles, allowing them to navigate the intercellular lipid matrix of the stratum corneum more easily [6].

Spironolactone (SPL) is an aldosterone blocker that also has antiandrogen effects. It works by inhibiting 5α-reductase activity, increasing testosterone clearance through enhanced liver hydroxylase activity. Topical spironolactone may provide similar benefits with fewer side effects. However, few studies have evaluated its effectiveness in treating acne. In this research, we aim to assess the safety and effectiveness of 0.25% topical spironolactone gel for managing acne vulgaris [7].

The term "Gel" was introduced to describe certain semisolid materials based on their physiological properties rather than their molecular makeup. Gels consist of a highly dilute, cross-linked network that remains solid-like in steady state. They comprise a two-part structure with a significant amount of liquid. A key feature of gels is the presence of a continuous matrix that exhibits solid-like behavior. Thanks to their biocompatibility, network architecture, and the stability of molecular bioactive agents, gels are commonly used in drug delivery applications [8].

MATERIAL AND METHODS

Material

Spironolactone Zhejiang Shenzhou Pharmaceutical Co., Ltd., China. Carbapol 934. Alpha Chemika, India; Cholesterol Bide Pharma Tech Co., China; Dialysis Membrane 8000-14000 Special Products Laboratory, USA; Soybean lecithin, Shaanxi Dideu Medichem Co., Ltd. China.

Methods

Preparation of Transethosomes

Ethanol injection method

Lecithin of different weights was dissolved with drug and cholesterol in ethanol (4 g) using

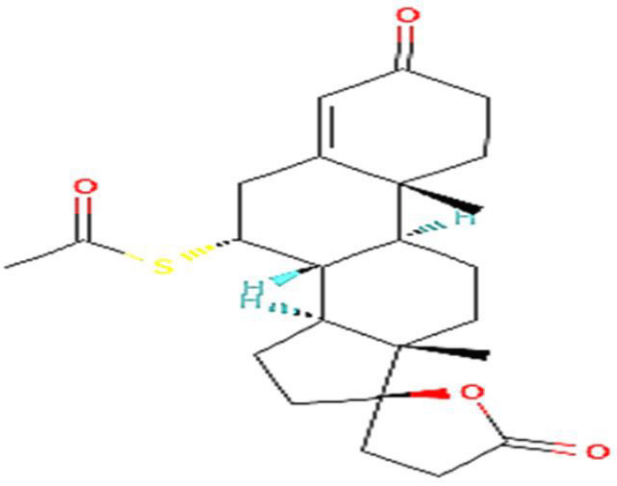


Fig. 1. Chemical structure of Spironolactone.

CC BY

bath sonication at 35°C for 5 min to produce the organic phase, as shown in Table 1. Following vesicle formation, approximately 1 g of ethanol was evaporated, resulting in a final ethanol content of 3 g. An aqueous phase comprised of water (up to 10 g). According to the composition of each formulation, a single edge activator was incorporated, Tween 80, when used dissolved in the aqueous phase, where Span 80 and sodium deoxycholate were dissolved in the organic phase, and the organic phase was added dropwise using a syringe at a 1 ml/min rate at 45°C to the aqueous phase while continuously stirred at 800 rpm to ensure uniform mixing. The mixture was stirred for 45 min for a smaller vesicular transethosomal dispersion [8].

Cold method

Spironolactone (SL), Phospholipon® 90G and cholesterol were dissolved in 4g ethanol as solvent using bath sonication at 30°C. An edge activator was incorporated in the ethanolic phase either as Span 80 or sodium deoxycholate depending on the composition of the formulation, while Tween 80, when used, was dissolved in the aqueous phase. The aqueous phase was made up with distilled water, the amount of which was adjusted to give a total weight of 10 g. The aqueous phase was then added slowly to the ethanolic phase using a 23-gauge syringe at a controlled rate of 1 mL/min under constant magnetic stirring at 800 rpm in a glass vessel. The stirring was continued for forty-five minutes. Therefore, the bottle was left open at room temperature for 24 h to allow the evaporation of approximately 1 g of ethanol [9].

Characterization of Trasethosomes

Particle size determination (PS)

PS and (PDI) of TEs were measured using the dynamic light scattering technique with the Malvern Zetasizer Nano ZS device (Malvern Instruments, Worcestershire, UK [10]. The effect of the type of surfactant, weight and type of phospholipids, method of preparation, and weight of the added cholesterol on the particle size and PDI were studied.

Encapsulation Efficiency (EE%)

The free SPL concentration in the TEs globule was used to indirectly determine the encapsulation efficiency (EE%) (Eq. 1) [11].

EE%=(total drug in formula-amount of free drug)/(total drug in formula)× 100%

Zeta Potential Measurement

The electrophoretic mobility of a prepared formula was assessed using the Malvern Zetasizer Nano ZS device (Malvern Instruments, Worcestershire, UK). This measurement was then converted to zeta potential, which indicates the extent of repulsion among charged particles

Table 1. SPL Transehosomes components.

Formula No.	Formula Code	Drug (mg)	Tween 80 (mg)	Span 80 (mg)	Sod.Deoxycholate/ Sodium Cholate (mg)	Phospholipid Type	Phospholipid Weight (mg)	Cholesterol (mg)	Ethanol (G)	Water (G)
1	SPL1	50	_	_	100	Lecithin	200	0	3	q.s to 10
2	SPL2	50	_	_	100	Lecithin	200	50	3	q.s to 10
3	SPL3	50	_	_	100	Lecithin	200	100	3	q.s to 10
4	SPL4	50	_	_	100	Lecithin	300	0	3	q.s to 10
5	SPL5	50	_	_	100	Lecithin	300	50	3	q.s to 10
6	SPL6	50	_	_	100	Lecithin	300	100	3	q.s to 10
7	SPL7	50	_	100	_	Lecithin	200	0	3	q.s to 10
8	SPL8	50	_	100	_	Lecithin	200	50	3	q.s to 10
9	SPL9	50	_	100	_	Phospholipon 90 g	200	100	3	q.s to 10
10	SPL10	50	_	100	_	Lecithin	300	0	3	q.s to 10
11	SPL11	50	_	100	_	Lecithin	300	50	3	q.s to 10
12	SPL12	50	_	100	_	Lecithin	300	100	3	q.s to 10
13	SPL13	50	100	_	_	Lecithin	200	0	3	q.s to 10
14	SPL14	50	100	_	_	Phospholipon 90 g	200	50	3	q.s to 10
15	SPL15	50	100	_	_	Lecithin	200	100	3	q.s to 10
16	SPL16	50	100	_	_	Lecithin	300	0	3	q.s to 10
17	SPL17	50	100	_	_	Lecithin	300	50	3	q.s to 10
18	SPL18	50	100	_	_	Lecithin	300	50	3	q.s to 10

CC BY

and evaluates the stability of the dispersion. The sample was placed into an electrophoretic cell by applying an electric field with a voltage of 15.2 V/cm [12].

Dissolution study

using USP dissolution apparatus II. According to BP specifications, the dissolution medium was 200mL with 0.5% SLS of phosphate buffer pH 5.5, maintained at 37 ± 1 C, and the paddle speed was 100 rpm. 2 ml samples were withdrawn at time intervals of 10min, 15min, 20min, 1hr, 2hr, 3hr, 4hr, 5hr, 7hr, 9hr, 12hr, 14hr, and 24hr, and the withdrawn samples were replaced with equal volumes of the dissolution medium. The drug content in each withdrawn sample was determined using a UV/Vis spectrophotometer at 242 nm [13].

Mathematical Modeling of Drug Release

Various kinetic models, including zero-order, first-order, and Higuchi plots, were used to analyze the dissolution data following the in vitro study. The model fit was assessed by comparing R2 values; the model with the highest R2 most accurately described the drug release process. Zero-Order Model: This method allows researchers to measure pharmaceutical release from osmotic systems, matrix tablets with poorly soluble drugs, and transdermal patches. The Eq. 2 characterizes drug release across various forms.

$$Ct = C0 + K_0 t$$

First-Order Model: Assuming first-order kinetics, Eq. 3 describes drug release from porous matrices with water-soluble drugs.

$$Log\ C = Log\ C_0 – Kt/2.303$$

Higuchi Model: It was the initial mathematical model designed to describe drug release from a matrix tablet. The model is based on specific assumptions regarding how drug release occurs in matrix systems. Its mathematical expression is given by the Eq. 4.

$$Ft = Q = A\sqrt{D}(2Cs) * Cst$$

Korsmeyer-Peppas Model: This model describes drug release from a polymeric system. To determine the drug-release mechanism, the first 60% of drug-release data was fitted to the Korsmeyer-Peppas model (Eq. 5).

$$Ct/C = Ktn$$

Drug-excipients compatibility study

FTIR analysis was performed on SPL, PM, and optimized TEs SPL using a Shimadzu Europe FTIR-8400S spectrophotometer. The spectra were obtained using the KBr pellet technique, which involves mixing the sample with dry KBr. Scanning covered a wavenumber range of 4000–200 cm^{-1} [14-16].

Powder X-ray diffraction (PXRD)

The purpose of PXRD is to analyze the drug's crystalline structure and detect physical changes during formulation. Therefore, tests were conducted on pure TEs and optimized formulation. The study utilized a powder X-ray diffractometer operating at 30 kV and 20 mA, with a continuous scan range of 2θ from 10 to 50 [17].

Differential Scanning Calorimetry (DSC)

The thermal behavior of pure SPL, Lecithin, and the optimized formula was studied with DSC (DSC-60 by Shimadzu, Japan). A 5 mg sample was sealed in an aluminum pan and heated from 25 to 250 °C at 10 °C/min under a nitrogen flow of 50 mL/min. The thermograms were analyzed using Origin 2026b (OriginLab Corporation, Northampton, MA, USA) [18, 19].

Table 2. Composition of spironolactone gel.

Formula code	Gelling agent	Percent
G1	CMC	0.5%
G2	CMC	1%
G3	Carbapole	1%

CC BY

Scanning electron microscopy (SEM)

Scanning electron microscopy was used to examine the morphology of the optimized formulation. The dried samples were dispersed onto aluminum stubs for morphological characterization. These samples were coated with a thin layer of gold and observed under an argon atmosphere using a scanning electron microscope operated at 30 kV. Representative images were then captured [20].

Preparation of gel

Carboxymethyl cellulose (CMC) was first dissolved in deionized water and stirred at 30 ◦C until completely solubilized to prepare 1% and 2% CMC stock solutions. Then, it was stored in a refrigerator for 24 hr to form a gel; the transethosomes formula (SPL13) was added gradually to the gel to form a spironolactone hydrogel, as shown in the Table 2 [21]. 0.1% methylparaben was added as a preservative.

Characterization of SPL-TEs based gel

Clarity and appearance

Clarity is considered one of the most essential features of gel. This test was performed under good lighting with a black-and-white background. The focus was on color, turbidity, and suspended particles [22].

pH of Gel

A digital pH meter was used to measure the pH of the prepared gel at room temperature, 2g of gel was dissolve in 50 ml distil water and left a side for 1hr. The measurement of pH of each formulation was triplicated and average values of pH were calculated [23, 24].

Determination of Viscosity and rheological properties

The rheological characteristics of the produced gel formulations were analyzed using a Myr digital viscometer (Model VR 3000, Spain). Initially, it was calibrated after balancing the surface. For the gel samples, shear tests were performed using an R6 spindle at 20, 50, and 100 rpm. Rheological behavior was inferred from plots of shear stress (rpm) versus viscosity (cP) [25].

Determination of SPL-gel Drug Content

To determine the drug content, take a required quantity of the prepared gel equivalent to 5mg of SPL and add it to a 50 mL volumetric flask; then add ethanol to the mark. Stir on a magnetic stirrer for 30 min to dissolve SPL, then filter and properly dilute with ethanol. SPL content was estimated

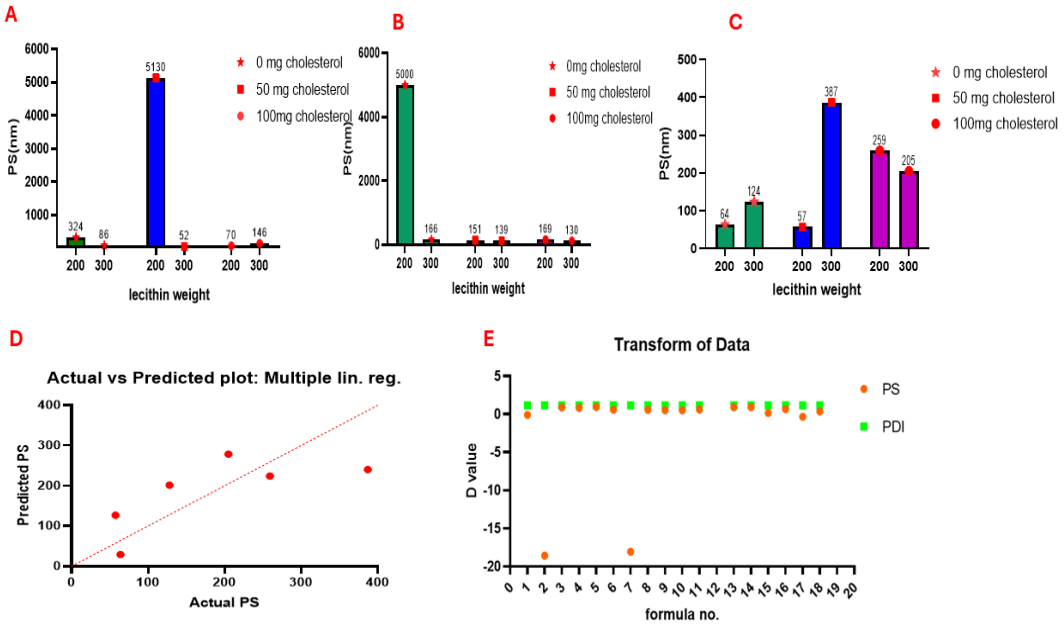


Fig. 2. Factors affecting PS of SPL transethosomes.

using a UV-Visible spectrophotometer at 238nm [26].

In vitro Dissolution Test

USP Apparatus 5 (Paddle-over-Disk Apparatus; in the Paddle-over-Disk method, the paddle and vessel assembly from Apparatus 2 was used with the addition of a disk assembly designed for holding the gel system at the bottom of the vessel) [27, 28] was used to assess the release pattern of SPL from the gel. The selection of apparatus for in vitro dissolution testing of dosage forms depends on various factors, including formulation, manufacturing process, drug properties such as solubility and diffusion, the method or apparatus employed in the assay, the dissolution medium, and the route of administration. The dissolution test was conducted at 37 °C in phosphate-buffered saline (200 mL, pH 5.5) at 100 rpm. 50mg of SPL gel was evenly spread on a Petri dish and formed into a gel in the dissolution medium. A 2 cm gap was maintained between the plate and the paddle. Samples (2 mL) were withdrawn and replaced with fresh buffer at 5, 10, 15, 30, 45, and 60 minutes to maintain sink conditions SPL content was estimated using a UV-Visible spectrophotometer at 241nm [29].

Determination of SPL gel Permeation

The experiments were conducted in three independent vertical Franz cells (A, B, and C) with a nominal volume of the acceptor compartment of 25 mL of 0.5 %sls phosphate-buffered (pH 7.4) and a diffusion area of 2.5 cm^2. For the donor compartment, the membrane was rat skin; a gel containing 5 mg of SPL was initially set and incubated at 37 °C and 100 rpm for 12 h. Samples were evaluated at different time points [30, 31].

Stability study of the prepared SPL-TEs and gel loaded with SPL-TEs.

The influence of temperature on the stability of the optimum SPL-TEs formula and the gel loaded with SPL-TEs of the optimum SPL-TEs formula was studied by storing samples at two temperatures (50ºC and room temperature) for two months. For SPL-TEs, particle size was evaluated at the end of two months. The drug content in SPL-TE-loaded gels was determined every two weeks. In addition, the effects of temperature on drug content of the prepared gel were studied after two months of storage at room temperature and 50ºC for the optimum formula.

Statistical analysis

The experimental data are presented as the mean and standard deviation (SD) for each sample and were analyzed using a one-way analysis of variance. Statistical significance was set at $P \leq 0.05$ and determined using SPSS version 26 and GraphPad Prism 8 software [32].

RESULTS AND DISCUSSION

Particle size, PDI, and EE%

The transethosomes encapsulated with SPL had a particle size (PS) between ~52.54 nm and 5000

Table 3. PS and PDI of SPL transethosomes.

Formula Cod	Surfactant	Phospholipid (mg)	Cholesterol (mg)	Ps (nm)	PDI	EE%
SPL1	Sod.deoxycholate/sodium cholate	200	0	324	0.5707	93±0.1
SPL2	Sod.deoxycholate/sodium cholate	200	50	5130	0.423	95±0.11
SPL3	Sod.deoxycholate/sodium cholate	200	100	70.1	0.1643	96.2±0.21
SPL4	Sod.deoxycholate/sodium cholate	300	0	86	0.2705	95.6±0.13
SPL5	Sod.deoxycholate/sodium cholate	300	50	52.54	0.1729	93±0.09
SPL6	Sod.deoxycholate/sodium cholate	300	100	146	0.135	95±0.12
SPL7	Span 80	200	0	5000	0.3807	99.4±0.10
SPL8	Span 80	200	50	151	0.248	98.9±0.22
SPL9	Span 80	200	100	169.1	0.2862	86±0.093
SPL10	Span 80	300	0	166	0.345	97±0.19
SPL11	Span 80	300	50	139	0.327	97±0.18
SPL12	Span 80	300	100	156	0.4686	92.8±0.12
SPL13	Tween 80	200	0	64	0.13	99±0.23
SPL14	Tween 80	200	50	57.47	0.2553	98±0.097
SPL15	Tween 80	200	100	259	0.427	99.4±0.22
SPL16	Tween 80	300	0	128	0.22	95.4±0.14
SPL17	Tween 80	300	50	387	0.377	29.8±0.18
SPL18	Tween 80	300	100	205	0.109	63±0.088

CC BY

nm. Table 3. The formulations produced vesicles of considerable variability in dimensions. Thus, particle size determination of the transethosomal system was based on the complex design, not only on cholesterol concentration.

SPL1–SPL6 formulations were formulated with sodium deoxycholate as an edge activator, resulting in a significant change in particle size. Variation in these formulations may be attributed to changes in the amount of sodium deoxycholate and cholesterol and the composition of phospholipids. The effect of cholesterol was not uniform across formulations suggesting that the effect of cholesterol on vesicle size and PDI is dependent on the interaction of cholesterol with other components of the vesicular system.

In SPL7–SPL12, the utilization of Span 80 as the edge activator led to variation in particle size due to changes in the concentrations of cholesterol and Span 80. The statistical analysis revealed that the differences in particle size observed were not significant statistically ($P > 0.05$). Thus, cholesterol should not be viewed as the only factor determining vesicle size, as its effect may depend on the type and concentration of edge activator and phospholipid used.

Formulations with tween 80 generally had particle sizes of less than 300 nm. Variations in particle size were seen in conjunction to different concentration of cholesterol. However

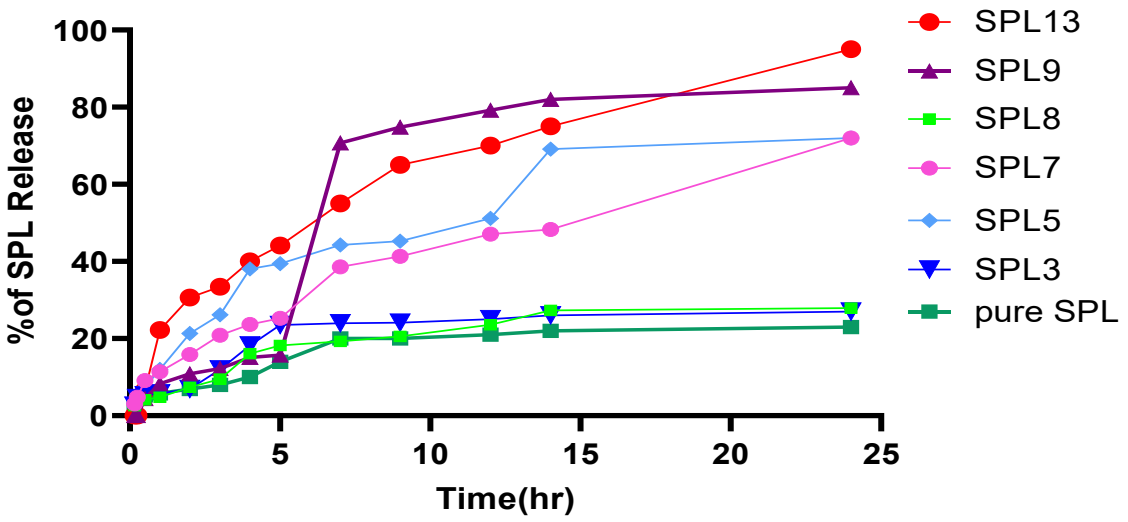


Fig. 3. SPL transethosome release.

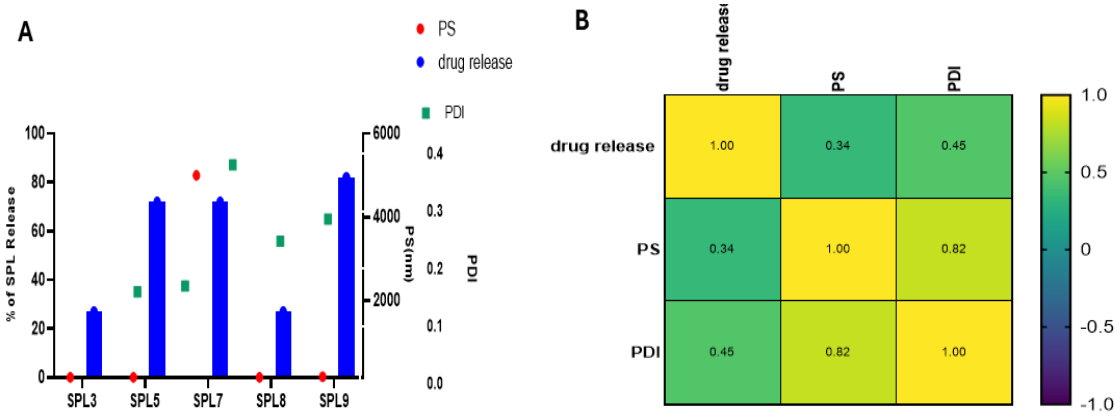


Fig. 4. Relationship between PS, PDI, and SPL release after 24 hr.

CC BY

these findings should be considered as overall effect of formulation parameters and not concentration dependent relationship with cholesterol. Cholesterol is integrated into the phospholipid bilayer and can change membrane structure, rigidity and vesicle formation. Thus, the physicochemical properties of the surfactant/ edge activator and the type and concentration of phospholipid incorporated in the formulation may finally control the effect on particle size [33, 34].

The results showed that the effect of cholesterol on the particle size and PDI of SPL-loaded transethosomes was dependent on the formulation. Rather, the final vesicular properties seem to be controlled by the balance between cholesterol, the nature and the amount of the edge activator and the phospholipid composition. Tween 80 transethosomes presented particle dimensions <300 nm, appropriate for topical medicinal delivery.

The transethosome formulation used the second method, the cold method, for a second phospholipid, phospholipone G90, which failed to form transethosomes by the ethanol injection method due to precipitation, as shown in Table 1. This method was used for SPL9 and SPL14, where the method had no effect on PS (P-value > 0.05). Encapsulation efficacy ranged from 22% to 99%.

In Vitro Drug Release

The in vitro release profile of the SPL transethosomal formulation was compared with that of the neat drug for SPL3 and SPL5, which contain sodium deoxycholate as a surfactant, and the particle size was 70nm and 50nm respectively (Fig. 4A show the relationship between PS, PDI,

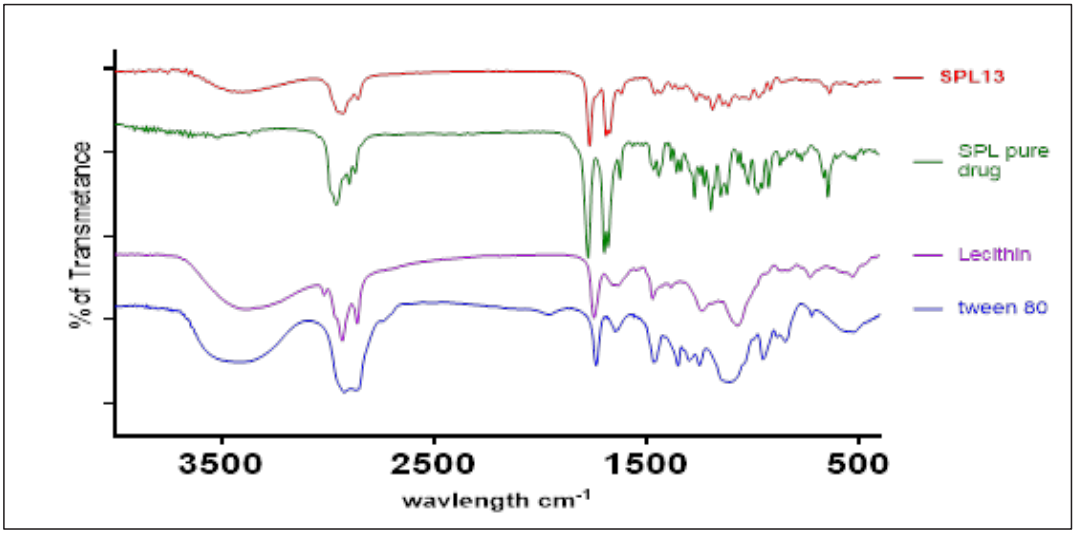


Fig. 5. FTIR of SPL, SPL23, lecithin and Tween.

Table 4. Mathematical Modeling of Drug Release.

Formula code	First order		Zero order		Ferst order with Fmax			Korsmeyer-Peppas			Higuchi	
	K1	Rseq	K0	R seq	K1	F max	R seq	kKP	n	R seq	KH	R seq
SPL3	0.057	0.9511	3.582	0.8129	0.088	76.832	0.9649	10.938	0.588	0.9908	13.512	0.9774
SPL5	0.021	0.6380	1.691	0.4901	0.177	28.088	0.9680	7.277	0.461	0.9433	6.641	0.9393
SPL7	0.101	0.8742	5.007	0.7394	0.088	108.943	0.8764	12.069	0.680	0.8239	18.583	0.7835
SPL8	0.023	0.3863	1.768	0.1871	0.257	27.168	0.9498	9.110	0.395	0.8723	7.134	0.8364
SPL9	0.078	0.9092	4.100	0.6202	0.152	70.894	0.9626	15.933	0.499	0.9596	15.901	0.9596
SPL13	0.106	0.9516	4.996	0.7195	0.124	92.402	0.9542	17.650	0.534	0.9765	19.142	0.9741

CC BY

and SPL release) for SPL3 contains 100 mg of cholesterol in its composition, that retarred its release (27%in 24 hr.), whereas SPL5 contains 50 mg of cholesterol in its composition, that highly significant enhance SPL release to reach 72% in 24 hr. (P<0.05) as shown in Fig. 2A, and Fig. 4B show the heat figure show the relationship between PS, PDI, and SPL release For SPL7, SPL8 and SPL9, which contain Span 80 as an edge activator, in the case of Span 80, SPL release was shown to behave differently; SPL7 (0 mg cholesterol) show 70% of SPL release, SPL 8(50 mg cholesterol) showed 27% that due to the presence of cholesterol stiffens the lipid tubules and diminishing their undulations along the axis. As cholesterol concentration increases, lattice-plane spacing enlarges and the water core diameter expands, while undulations along the lipid tubule axis decrease [17]; SPL9 (100 mg cholesterol) showed highly significant drug release (85% in 24 hr). For SPL13, drug release was 95% in 24 hr, which is highly significant (P< 0.05) in comparison with other formulations.

Mathematical Modeling of Drug Release

Drug release models are shown in Table 4, in which R seq was calculated; based on R seq, Korsmeyer was the best-fit model, with drug release predominantly following an anomalous(on-fickian) transport mechanism, indicating that both diffusion, cholesterol weight, and phospholipid

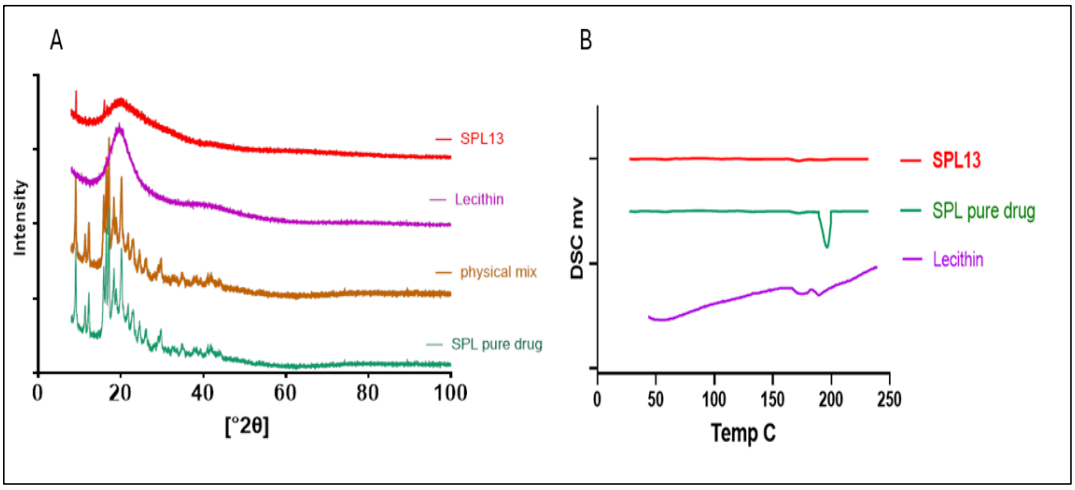


Fig. 6. (A) PXRD of SPL, SPL23, lecithin and physical mixture (B) DSC of SPL, SPL13, and lecithin.

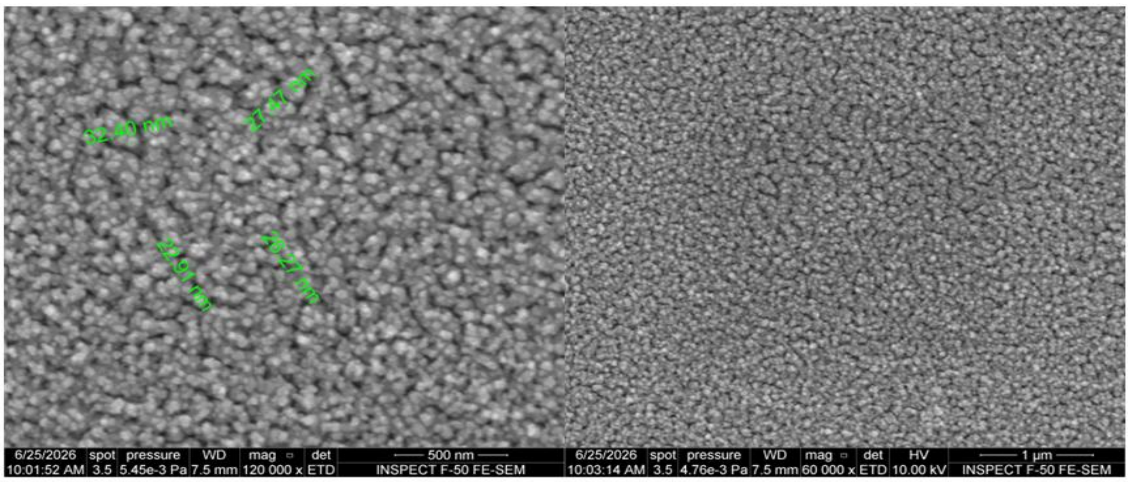


Fig. 7. Morphology of SPL13 by SEM.

weight contribute to SPL release.

Drug-excipients compatibility study

FTIR spectrum studies indicated that major functional groups present in Spironolactone show characteristic peaks in the IR spectrum. The major peaks match the functional groups of Spironolactone. Hence, it was confirmed that there was compatibility between the drug and various excipients. The pure Spironolactone spectrum showed sharp peaks at wavenumbers 1617 (-C=C stretching of the α, β-unsaturated ring), 1673(-C=O stretching of α, βunsaturated ring), 1768(-C=O stretching of the thioacetyl group), 1791 (-C=O stretching of the lactone ring), and 2950 cm– 1 (-C=H stretching), as shown in Fig. 5 (35, 36). Spectra of lecithin show peaks from C = O stretching bonds in ester groups at 1,737 cm^{-1}, peaks from C-O stretching bonds at 1,376 and 1,227 cm^{-1}, and peaks from C- H bonds of fatty acid long chains at 2,852 and 2, 921 cm^{-1}[37, 38].

In the FTIR spectrum of Tween 80, a broad and strong band was observed in the range of 3100–3700 cm–1 due to the stretching vibrations of O–H. The bands at 1103 and 1738 cm–1 are respectively ascribed to the asymmetric C–O and C=O stretching vibrations [39]. The broad peak (3400 cm^{-1}) appeared in the SPL13 FTIR. This may be due to the formation of a new hydrogen bond. In addition, all other peaks of SPL were retained, indicating no chemical interaction. These results may indicate the development of nanovesicles with appropriate shape, size, and better stability, as reported in a previous study; see Fig. 5.

Solid-State characterization

Fig. 6A shows the XRD diffractogram of PL, SPL23, lecithin, and the physical mixture to analyze the solid form and the crystalline purity of SPR raw materials. SPL shows a characteristic peak, and the pure drug exhibits crystalline peaks at 2θ = 10.1 °, 13.2°, 14.6°, and 15.2° [40]. In contrast, the characteristic diffraction peaks of SPL13 were broad and blunt, indicating decreased crystallinity

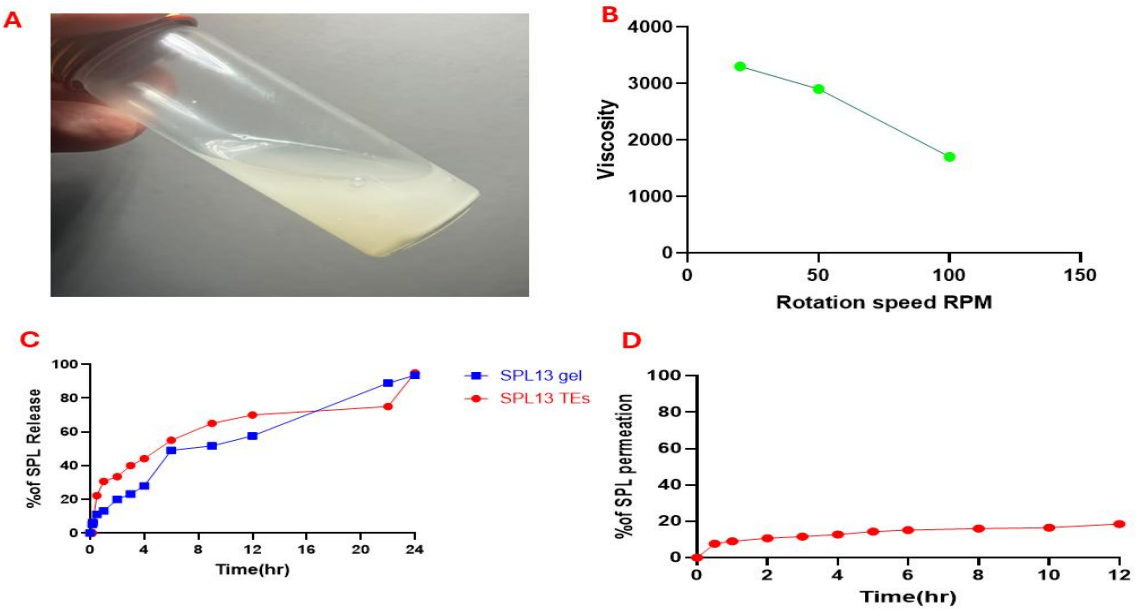


Fig. 8. characterization of SPL-TEs loaded gel.

Table 5. stability study of SPL-TEs loaded gel.

Temperature	Visual appearance	Drug content
25C	opaque and uniform	97%
50C	opaque and uniform	96.2%

CC BY

and the presence of amorphous material. The absence of the crystalline drug peaks confirms the amorphous state of the optimized formula. DSC thermogram of SPL (Fig. 6B) indicated a melting value of 204.5 °C. No melting point peak of SPL in SPL13 DSC was detected in the DSC thermogram, which confirms the formation of an amorphous form.

Scanning electron microscopy (SEM)

Vesicles were round, homogeneous, and smooth on the surface. SEM analysis also supported that the vesicle size was less than 100 nm.

Characterization of SPL-TEs-based Gel

Visual Appearance

The SPL gel formulas (G1 and G2) appeared opaque and uniform and had an optimal consistency Fig. 8A. Carbopol gel (G3) was full of bubbles. Base on visual appearance, G1 was selected as optimum formula that further characterized.

pH

The pH of the prepared gel was 6.4 ± 0.1, which falls within the acceptable skin-compatible range of 5–7. This minimizes the risk of skin irritation and ensures safe application [41].

Drug Content

The SpL content in the gel was measured at 99% ±1, demonstrating a uniform distribution throughout the gel matrix. This suggests effective formulation methods and stable SPL in the gel base [42].

Spreadability and Rheological Studies:

The rheological study shows pseudoplastic

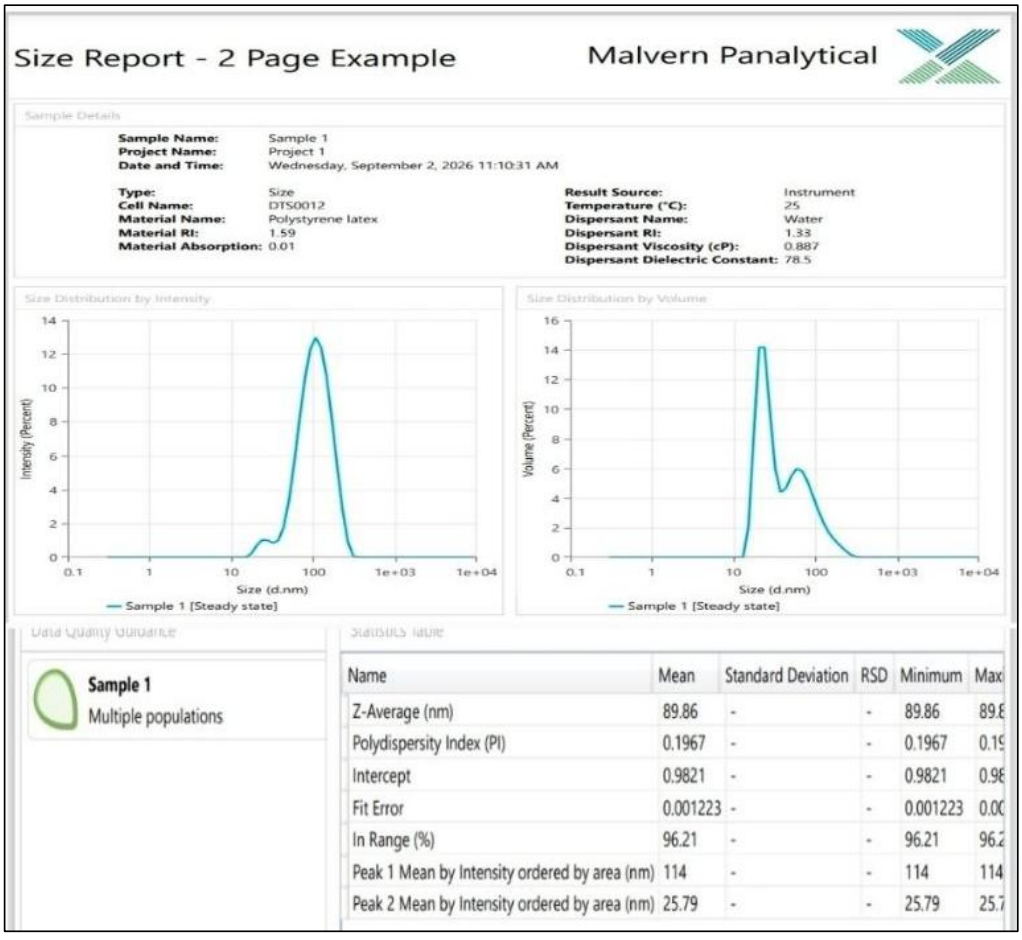


Fig. 9. PS and PDI of SPL13 formula after two months in room temperature.

flow, where higher shear rates reduce viscosity, as shown in the Fig. 8B.

In vitro release study of SPL-TEs Gel:

The in vitro release profile of SPL from the gel formulation, shown in Fig. 8C, demonstrated rapid drug release, reaching nearly 100% within the first 24 hr.

Permeation Study of SPL-TEs-loaded Gel

Penetration of only 18% in 12 hr, indicating SPL entrapment in the skin rather than penetration through the skin to systemic circulation, as shown in Fig. 8D, and flux was calculated to be (Flux= 15.21 mcg/cm2/hr).

Stability study of TEs and Gel

For TEs, the stability study was confirmed by measuring PS after two months at room temperature, as shown in Fig. 9. The PS was less than 100 nm (89.8 nm) with a PDI of 0.196. The second peak appears due to small particle aggregates in the 1:0.25 fraction. Stability of SPL-TEs was assessed by visual appearance, viscosity, and drug content, as summarized in Table 5.

CONCLUSION

Our research demonstrated effective trapping of SPL within TEs composed of lecithin or Phospholipon 90G as phospholipids, Tween 80, sodium deoxycholate and Span 80 as edge activators and cholesterol at different weights. We examined and validated the entrapment, stability, and morphology of SPL-TES using several analytical techniques, including FT–IR, XRD, DSC, and FESEM. This finding corroborates and correlates with current research endeavors in the domain of TEs as a medication delivery method. Gel was prepared using CMC as a gelling agent and was successfully prepared.

CONFLICT OF INTEREST

The authors declare that there is no conflict of interests regarding the publication of this manuscript.

REFERENCES

1. Shanta Taher S, Sadeq ZA, Al-Kinani KK, Alwan ZS. Solid Lipid Nanoparticles as a Promising Approach for Delivery of Anticancer Agents: Review Article. Military Medical Science Letters. 2022;91(3):197-207.
2. Jassim ZE, Mohammed MF, Sadeq ZA. Formulation and Evaluation of Fast Dissolving Film of Lornoxicam. Asian Journal of Pharmaceutical and Clinical Research. 2018;11(9):217.
3. Sadeq ZA. Review on Nanoemulsion: Preparation and Evaluation. International Journal of Drug Delivery Technology. 2020;10(01):187-189.
4. Bin Jardan YA, Ahad A, Raish M, Al-Jenoobi FI. Preparation and Characterization of Transethosome Formulation for the Enhanced Delivery of Sinapic Acid. Pharmaceutics. 2023;15(10):2391.
5. Malang SD, Shambhavi, Sahu AN. Transethosomal gel for enhancing transdermal delivery of natural therapeutics. Nanomedicine. 2024:1-19.
6. Mohd H, Dopierała K, Zidar A, Virani A, Michniak-Kohn B. Effect of Edge Activator Combinations in Transethosomal Formulations for Skin Delivery of Thymoquinone via Langmuir Technique. Sci Pharm. 2024;92(2):29.
7. Ayatollahi A, Samadi A, Bahmanjahromi A, Robati RM. Efficacy and safety of topical spironolactone 5% cream in the treatment of acne: A pilot study. Health Science Reports. 2021;4(3).
8. Bhuyan C, Saha D, Rabha B. A Brief Review on Topical Gels as Drug Delivery System. Journal of Pharmaceutical Research International. 2021:344-357.
9. Farooq M, Usman F, Zaib S, Shah HS, Jamil QA, Akbar Sheikh F, et al. Fabrication and Evaluation of Voriconazole Loaded Transethosomal Gel for Enhanced Antifungal and Antileishmanial Activity. Molecules. 2022;27(10):3347.
10. Noor NA, Al-Gawahri F. Ophthalmic Single and Mixed Polymeric Nanomicelles using Brimonidine as a model drug: Preparation, Characterization, and Physical Properties Evaluation. Iraqi Journal of Pharmaceutical Sciences. 2025;34(3):202-214.
11. Hala Mohammed F, Ahmed KK. Formulation and Evaluation of Lercanidipine HCL Loaded Nanomicelles. Iraqi Journal of Pharmaceutical Sciences. 2026;35(1):80-88.
12. Ibrahim Ahmed A, Rajab NA. MIRTAZAPINE LOADED PRONANOMICELLES: PREPARATION AND CHARACTERIZATION. International Journal of Applied Pharmaceutics. 2026:283-291.
13. Elkordy AA, Tan XN, Essa EA. Spironolactone release from liquisolid formulations prepared with Capryol™ 90, Solutol® HS-15 and Kollicoat® SR 30 D as non-volatile liquid vehicles. Eur J Pharm Biopharm. 2013;83(2):203-223.
14. Nizar Awish J, Shaimaa Nazar Abd A. Formulation and Evaluation of Canagliflozin Self-nanomicellizing Solid Dispersion Based on Rebaudioside A for Dissolution and Solubility Improvement. Iraqi Journal of Pharmaceutical Sciences. 2025;33((4SI)):43-56.
15. Etodolac Topical Spray Films, Development, Characterization and In-Vitro Evaluation. International Journal of Pharmaceutical Research. 2020;12(04).
16. Sadeq ZA, Mohammed MF. Preparation and in vitro evaluation of topical gel of 5-fluorouracil. Journal Of Advanced Pharmacy Education And Research. 2021;11(4):80-85.
17. Amal Abdullah M, Shaimaa Nazar Abd A. Preparation, In Vitro Evaluation and Characterization studies of Clozapine Nanosuspension. Iraqi Journal of Pharmaceutical Sciences. 2025;33((4SI)):336-348.
18. Mohammed MF, Sadeq ZA, Salih OS. Formulation and evaluation of mucoadhesive buccal tablet of Anastrozole. Journal Of Advanced Pharmacy Education And Research. 2022;12(2):38-44.

CC BY

19. Ahmed Sadeq Z, Abdalkarim Sabri L. Formulation and Optimization of Soluplus® /Poloxamer 338-Based Repaglinide Nanomicelles Using Box-Behnken Design. International Journal of Applied Pharmaceutics. 2026.
20. Milad Jawad H, Nawal Ayash R. Tizanidine Cubosomal Nano Carriers as Transdermal Delivery System: Preparation and Characterization. Iraqi Journal of Pharmaceutical Sciences. 2026;35(2):50-65.
21. Wang J, Zhang Z, He X, Gao B. Preparation and Properties of CMC-Based Composite Gel as a Flame-Retardant Dust Suppressant. Gels. 2026;12(9):755.
22. Parmar N, Sharma R, Patel J, Khan S, Patel R. FORMULATION AND EVALUATION STUDIES OF VALACYCLOVIR TOPICAL GEL FOR ANTIVIRAL ACTIVITY. International Journal of Pharmaceutical Sciences and Medicine. 2022;7(10):97-118.
23. Lalithajyotsna N, Sarfaraz Ali Ahmed M, choudary M, Bakshi Dv. Formulation and Evaluation of Antimicrobial Activity of Topical Niosomal Gel of ErythromycinFormulation and Evaluation of Antimicrobial Activity of Topical Niosomal Gel of Erythromycin. American Journal of Pharmacy And Health Research. 2018;6(6):27-38.
24. Lakhe E. In -Vitro Assessment Of Anti-Inflammatory Activity Of Ethanolic Extract Of Fenugreek Seeds And Demonstration Of Effectiveness In Animal Models (In- Vivo) Through Characterization Of Gel Formulation Containing The Extract. International Journal of Scientific and Research Publications (IJSRP). 2021;11(6):571-585.
25. Sadeq ZA, Sabri LA, Al-Kinani KK. Natural polymer Effect on gelation and rheology of ketotifen-loaded pH-sensitive in situ ocular gel (Carbapol) ⁋. Journal Of Advanced Pharmacy Education And Research. 2022;12(2):45-50.
26. Kaundal N, Kumar P. Formulation and Evaluation of Ethosomal Cream containing Resveratrol for the Treatment of Contact Dermatitis. Journal of Drug Delivery and Therapeutics. 2024;14(5):49-63.
27. Prodduturi S, Sadrieh N, Wokovich AM, Doub WH, Westenberger BJ, Buhse L. Transdermal delivery of fentanyl from matrix and reservoir systems: Effect of heat and compromised skin. J Pharm Sci. 2010;99(5):2357-2366.
28. Qiu S, Wang K, Li M. In Vitro Dissolution Studies of Immediate-Release and Extended-Release Formulations Using Flow-Through Cell Apparatus 4. Dissolution Technologies. 2014;21(2).
29. Malik B, Bekir E. Formulation and in vitro /in vivo Evaluation of Silymarin Solid Dispersion- Based Topical Gel for Wound Healing. Iraqi Journal of Pharmaceutical Sciences (P-ISSN 1683 - 3597 E-ISSN 2521 - 3512). 2023;32(Suppl.):42-53.
30. Salamanca CH, Barrera-Ocampo A, Lasso JC, Camacho N, Yarce CJ. Franz Diffusion Cell Approach for Pre-Formulation Characterisation of Ketoprofen Semi-Solid Dosage Forms. Pharmaceutics. 2018;10(3):148.
31. Seo J-E, Kim S, Kim B-H. In vitro skin absorption tests of three types of parabens using a Franz diffusion cell. Journal of Exposure Science and Environmental Epidemiology. 2016;27(3):320-325.
32. Wu J, den Mooter GV. Statistical analysis of long-term physical stability testing of amorphous solid dispersions. Int J Pharm. 2025;681:125844.
33. Sarotsumpan P, Chiu IH, Wu P-C, Khong N, Liew C, Chutoprapat R. Development and Evaluation of Trans-Resveratrol-Loaded Transfersomes: Role of Cholesterol in Formulation Design for Dermal Delivery. Nanotechnology, Science and Applications. 2025;Volume 18:359-375.
34. Choi S, Kang B, Yang E, Kim K, Kwak MK, Chang P-S, et al. Precise control of liposome size using characteristic time depends on solvent type and membrane properties. Sci Rep. 2023;13(1).
35. Akbari J, Saeedi M, Morteza-Semnani K, Kelidari HR, Sadegh Moghanlou F, Zareh G, et al. The Effect of Tween 20, 60, and 80 on Dissolution Behavior of Sprionolactone in Solid Dispersions Prepared by PEG 6000. Advanced Pharmaceutical Bulletin. 2015;5(3):435-441.
36. Chandrasekaran P. Nanocrystal-Based Solid Oral Flexible Formulation Platform for Pediatric and Geriatric Drug Delivery. Morressier; 2016.
37. Nzai JM, Proctor A. Soy lecithin phospholipid determination by fourier transform infrared spectroscopy and the acid digest/arseno-molybdate method: A comparative study. J Am Oil Chem Soc. 1999;76(1):61-66.
38. Michał W, Ewa D, Tomasz C. Lecithin-based wet chemical precipitation of hydroxyapatite nanoparticles. Colloid Polym Sci. 2015;293(5):1561-1568.
39. Bide Y, Fashapoyeh MA, Shokrollahzadeh S. Structural investigation and application of Tween 80-choline chloride self-assemblies as osmotic agent for water desalination. Sci Rep. 2021;11(1).
40. Demirturk E, Gundogdu G, Cetin M, Bilensoy E. Improved Bioavailability of Spironolactone–Hydroxypropyl-β-Cyclodextrin Complex Tablets Evaluated in Rat Model. J Pharm Innov. 2026;21(5).
41. Schlich M, Lai F, Maria Fadda A, Sinico C, Pini E. Drug-Excipients Compatibility Studies in Proniosomal Formulation: A Case Study with Resveratrol. Journal of Nanoscience and Nanotechnology. 2021;21(5):2917-2921.
42. Herneisey M, Williams J, Mirtic J, Liu L, Potdar S, Bagia C, et al. Development and Characterization of Resveratrol Nanoemulsions Carrying Dual-Imaging Agents. Ther Deliv. 2016;7(12):795-808.

CC BY